Selection of Catalysts through Cellular Reproduction

Naoaki Ono[1] and **Takashi Ikegami**[2]

[1]ATR, Human Information Science Laboratories, 2-2-2Hikaridai,
"Keihanna Science City" (Seika-cho, Soraku-gun), Kyoto 619-0288, Japan
[2]Institute of Physics, Graduate School of Arts and Sciences,
University of Tokyo, 3-8-1 Komaba Tokyo 153-8902, Japan

Abstract

A series of simulation studies (Ono & Ikegami 1999; 2001) show that a proto cell spontaneously emerges from a chemical soup by acquiring membrane structures. In 2-dimensional space, the emergence of proto cells is followed by the reproduction of cells. A major unsolved problem is the evolution of proto cells; how the proto cells evolve into modern cells with higher functionalities. Here we examine, as the first step, the evolution of catalysts within the proto-cells. Catalytic chemicals have different catalytic activity in generating membrane chemicals. We show that cells with higher activity of membrane production evolve through cellular selection.

Introduction

It is widely accepted that the origin of life was a set of molecules that catalyzed the reproduction of each other. However, when we consider the evolution of such primitive chemical systems, the compartmentalization of molecules is indispensable for establishing the co-evolution of cooperative catalytic reactions and protecting them from parasites that would spoil the evolution (Szathmáry & Maynard Smith 1997). Though it is difficult to know about the structure of primitive cells because there remain few physical records of the earliest living cells, there have been various theoretical approaches to understanding the emergence and evolution of proto-cell systems.

Gánti proposed a minimal model of primitive self-maintaining cells named "chemoton" (Gánti 1975; 1997). It is composed of (1) a metabolic system of autocatalytic molecules, (2) self-replicating molecules that inherit genetic information and (3) a self-organizing membrane molecule to enclose the whole system. This system maintains itself by consuming resources and discharging waste into the environment. It can be easily imagined that if the reproduction of the cell is appended to this system, it would be a primitive unit of Darwinian selection and evolve into more stable structures.

It should be stressed that a cell defines itself as an individual by producing a membrane that distinguishes itself from the outside. Maturana and Varela pointed out that this is a unique feature of living organisms, and named it "autopoiesis" (Maturana & Varela 1980). To demonstrate the self-maintenance of an autopoietic structure, abstract computational models of an autopoietic cell based on a Cellular Automaton were proposed (originally by Varela (Varela, Maturana, & Uribe 1974), and re-implemented by Zeleny (Zeleny 1977) and by McMullin (McMullin & Varela 1997)). Breyer and McCaskill introduced the metabolism of a catalyst into this model (Breyer, Ackermann, & McCaskill 1998). It was also shown that an autopoietic proto-cell can reproduce itself automatically (Ono & Ikegami 1999; 2001). Speroni di Fenizio and Dittrich proposed another approach to represent proto-cells that are embedded in a triangular planar graph (Speroni di Fenizio, Dittrich, & Banzhaf 2001).

The remaining question is "How was the *first* cell organized?" Answering this question will give us the first step in understanding the emergence of higher order structures in life's evolution. This paper consists of two parts. The computational algorithm of the model is explained in detail in the first part. We introduce a Lattice Artificial Chemistry (LAC) model that simulates the chemical reactions and spatial interactions of abstract chemicals. In the second part, an emergence of a proto-cell from a non-organized initial state, its reproduction and the selection of inside catalysts through the cell reproduction are reported in order.

Lattice Artificial Chemistry

Our model is based on discrete and stochastic dynamics, which is extended from a lattice-gas model. Chemicals are represented by particles on reaction sites that are arranged as a two-dimensional triangular lattice. Note that any number of particles can be placed on a single site. The vector $\mathbf{n}(\mathbf{x}) = (n_1(\mathbf{x}), n_2(\mathbf{x}), \ldots, n_m(\mathbf{x}))$ gives the number of each type of particles on the site $\mathbf{x}$. N_i gives the total amount of i-th particles in the system.

Chemical reactions are expressed by the probabilistic transition of particle types. The diffusion of chemicals is expressed by random walks of particles on the sites. These transition probabilities are given as the products

of the associated rate coefficients and the following function of the potential change ΔE,

$$f(\Delta E) = \frac{\Delta E}{e^{\beta \Delta E} - 1}. \quad (1)$$

where β represents the inverse of the product of the Boltzmann constant and temperature (note that, $f(\Delta E)/f(-\Delta E) = e^{-\beta \Delta E}$). In the simulations reported hereafter, the value of β is normalized and fixed to 1.

Hydrophobic Interaction

The probabilities of random walks of particles are biased according to the gradient of the potential $\Psi(\mathbf{x})$ which is given by summing up the interaction from all particles in the same and adjacent sites. The probability p with which a particle i moves from a site $\mathbf{x}$ to $\mathbf{x}'$ is calculated as follows,

$$\Psi_i(\mathbf{x}) = \sum_{|\mathbf{x}'-\mathbf{x}| \leq 1} \sum_j \psi_{ij}(\mathbf{x}' - \mathbf{x}) n_i(\mathbf{x}) \quad (2)$$

$$p_i(\mathbf{x} \rightarrow \mathbf{x}') = Dif_i \, f(\Psi_i(\mathbf{x}') - \Psi_i(\mathbf{x})) \quad (3)$$

where $\Psi_i(\mathbf{x})$ denotes the potential of particle i in the site $\mathbf{x}$,Dif_i denotes the diffusion coefficient of particle i, and $\psi_{ij}(d\mathbf{x})$ denotes the interaction on particle i from particle j. Diffusion coefficients depend on the species of the particles. Autocatalytic and membrane particles are assumed to be larger molecules so that their diffusion coefficients are smaller than those of other particles ($Dif_{A_i} = Dif_M = 0.003$, $Dif_{others} = 0.01$).

To simulate the formation of membranes, we introduce hydrophobic interactions between particles. First, the particles are grouped into three classes: hydrophilic, hydrophobic and neutral. In general, all particles repel each other, but repulsion between hydrophilic and hydrophobic particles is much stronger than that between other particles so that phase separation between different classes of particles takes place. On the other hand, neutral particles do not repel other particles very strongly so that they can diffuse more freely.

Next, we assume that hydrophobic particles $\mathbf{M}$ are anisotropic. Namely, the repulsion around a particle $\mathbf{M}$ depends on its orientation and the configuration of the particles as illustrated in Fig. 1. There are specific directions in which the repulsion becomes strong, while the repulsion becomes weak in the other directions Taking its symmetry into account, a particle $\mathbf{M}$ can rotate to six different orientations ($\mathbf{M^0}$, $\mathbf{M}^{\pm\pi/6}$, $\mathbf{M}^{\pm\pi/3}$, $\mathbf{M}^{\pi/2}$) stochastically according to the gradient of the potential as follows,

$$p_{\mathbf{M}^{k \rightarrow k'}}(\mathbf{x}) = Rot \, f(\Psi_{\mathbf{M}^{k'}}(\mathbf{x}) - \Psi_{\mathbf{M}^k}(\mathbf{x})) \quad (4)$$

where $Rot = 0.01$ denotes the rotation coefficient. The repulsion between two particles $\mathbf{M}$ becomes strong when their orientations are different, so that they tend to align in the same orientation. According to these interactions, particles $\mathbf{M}$ gather together to form stretched clusters. We call these stretched structures of particle $\mathbf{M}$ "membrane". Though the characters of membranes, such as flexibility, depends on these values, the formation of membranes can be observed in a wide range of parameters. The detail values of repulsion $\psi_{ij}(d\mathbf{x})$ which are arbitrary chosen for the following experiments are listed in Tables 1a and 1b.

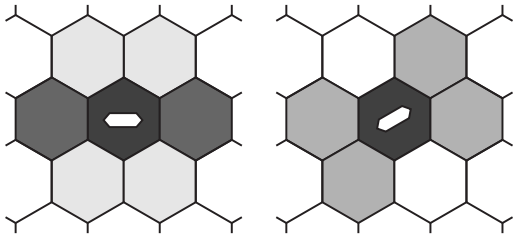

(a) $\mathbf{M^0}$ (b) $\mathbf{M}^{\pi/6}$

Figure 1: Illustration of repulsion around a particle $\mathbf{M}$. The honeycomb cells represent the lattice sites. The depth of gray shade corresponds to the magnitude of repulsion against a hydrophilic particle on the site from the particle $\mathbf{M}$ on the center site. The repulsion becomes stronger on the dark gray sites than on the light gray sites.

Table 1: a. Repulsion between isotropic particles.

particles		position	
		$dr = 0$	$dr = 1$
hydrophilic	hydrophilic	0.0100	0.0033
	neutral	0.0010	0.0003
neutral	neutral	0.0010	0.0003

Chemical Reaction

We introduce a simple metabolic system of autocatalytic particles. Consider that there are various species of self-replicating particles, and some of them have the ability to catalyze the production of membrane particles. Resources of these particles are supplied from some external source homogeneously.

Figure 2 illustrates the reaction paths. The probabilities of chemical reactions depend on the enthalpy change along with the transition, as follows,

$$\Delta H_{ij} = \Delta H_j - \Delta H_i \quad (5)$$

$$p_{i \rightarrow j}(\mathbf{x}) = k_{ij}(\mathbf{x}) \, f(\Delta H_{ij} + \Psi_j(\mathbf{x}) - \Psi_i(\mathbf{x})) \quad (6)$$

where ΔH_{ij} denotes the enthalpy change that is given by the difference in the formation enthalpy listed in Table 2.

Table 1.b Repulsion between hydrophobic and other particles

particles		position			
		$dr = 0$	$dr = 1$		
			$\theta = 0, \pi$	$\theta = \pi/3, -2\pi/3$	$\theta = 2\pi/3, -\pi/3$
$\mathbf{M^0}$	hydrophilic	0.2000	0.1600	0.0200	0.0200
	neutral	0.0010	0.0008	0.0001	0.0001
	$\mathbf{M^0}$	0.0100	0.0033	0.0033	0.0033
	$\mathbf{M^{\pi/6}}$	0.0777	0.0259	0.0259	0.0259
	$\mathbf{M^{\pi/3}}$	0.1433	0.0477	0.0477	0.0477
	$\mathbf{M^{\pi/2}}$	0.2100	0.0700	0.0700	0.0700
$\mathbf{M^{\pi/6}}$	hydrophilic	0.2000	0.1000	0.1000	0.0000
	neutral	0.0010	0.0005	0.0005	0.0000
	$\mathbf{M^{\pi/6}}$	0.0100	0.0033	0.0033	0.0033
	$\mathbf{M^{-\pi/3}}$	0.2100	0.0700	0.0700	0.0700

$k_{ij}(\mathbf{x})$ denotes the coefficient of reaction $i \leftrightarrow j$ that may depend on the number of catalysts on the site. Note that the effects of the interactive potential, namely, the effects of hydrophilic/hydrophobic environments are also taken into account here, therefore, for example, it becomes more difficult to synthesize a hydrophilic particle in a hydrophobic environment.

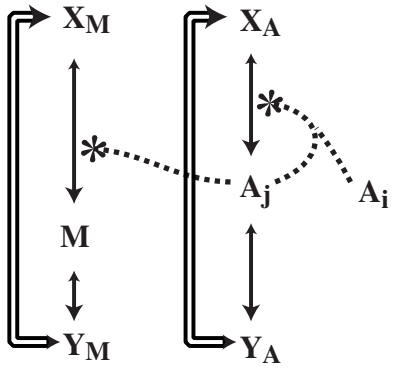

Figure 2: Schematic drawings of reaction paths. An autocatalyst ($\mathbf{A_i}$) catalyzes the reproduction of another particle $\mathbf{A_j}$ from a resource particle ($\mathbf{X_A}$) that has a higher chemical energy. It also catalyzes the production of a membrane particle ($\mathbf{M}$) from another resource particle ($\mathbf{X_M}$). All particles decay into waste particles ($\mathbf{Y_A}$ and $\mathbf{Y_M}$, respectively), spontaneously, however, an external energy supply recycles $\mathbf{Y_A}$ and $\mathbf{Y_M}$ into $\mathbf{X_A}$ and $\mathbf{X_M}$, respectively. The number of total particles is preserved.

Table 2: Formation enthalpy

particle	$\mathbf{X_A}$, $\mathbf{X_M}$	$\mathbf{A_i}$	$\mathbf{M}$	$\mathbf{Y_A}$, $\mathbf{Y_M}$
ΔH_i	12.0	6.0	4.0	0.0

There are ten species of autocatalytic particles ($\mathbf{A_0} \ldots \mathbf{A_9}$). An autocatalytic particle $\mathbf{A_i}$ catalyzes the replication of another particle $\mathbf{A_j}$ using it as a template and consuming a resource particle ($\mathbf{X_A}$).

$$\mathbf{A_i} + \mathbf{A_j} \quad \longleftrightarrow \quad \mathbf{A_i A_j} \tag{7}$$

$$\mathbf{A_i A_j} + \mathbf{X_A} \quad \longleftrightarrow \quad \mathbf{A_i A_j} + \mathbf{A_j} \tag{8}$$

There is a probability of mutation μ with which a particle $\mathbf{A_i}$ mutates to $\mathbf{A_{i\pm 1}}$ when it is reproduced. Assuming that the rate of the first reaction is much faster than that of the second one, the rate coefficients between $\mathbf{X_A}$ and $\mathbf{A_j}$ can be given as follows,

$$n'_{A_i}(\mathbf{x}) = \mu n_{A_{j-1}}(\mathbf{x}) + (1-2\mu) n_{A_j}(\mathbf{x}) + \mu n_{A_{j+1}}(\mathbf{x}) \tag{9}$$

$$k_{X_A \leftrightarrow A_j}(\mathbf{x}) \quad = \quad k_A + C_A n'_{A_i}(\mathbf{x}) \sum_i n_{A_i}(\mathbf{x}) \tag{10}$$

where $n_{A_i}(\mathbf{x})$ denotes the number of particles $\mathbf{A_i}$ on the site $\mathbf{x}$, and k_A denotes the rate of spontaneous reaction. Note that all autocatalysts share a common catalytic activity C_A and catalyze the replication of each other equally.

An autocatalytic particle also catalyzes the production of a membrane particle ($\mathbf{M}$) from a resource ($\mathbf{X_M}$). The activity (C_{M_i}) depends on the species. The catalytic activity of each species $\mathbf{A_i}$ is given by the following equation, namely, the activity of particle $\mathbf{A_i}$ is i-th times larger than that of particle $\mathbf{A_1}$, so that the rate coefficients between $\mathbf{X_M}$ and $\mathbf{M}$ are given as follows,

$$C_{M_i} \quad = \quad C_M \times i \tag{11}$$

$$k_{X_M \leftrightarrow M}(\mathbf{x}) \quad = \quad k_M + \sum_i C_{M_i} n_{A_i}(\mathbf{x}), \tag{12}$$

where C_M is a given constant, and k_M denotes the rate of spontaneous reaction.

These particles naturally decay into waste particles ($\mathbf{Y_A}$ and $\mathbf{Y_M}$, respectively) at a constant rate k_Y. However, we introduce an external source that supplies resources. To preserve the total number of particles, the resource supply is expressed by the exchange from waste

to resource particles.Thus the transition coefficients are given as follows,

$$k_{A_j \leftrightarrow Y_A} = k_{M \leftrightarrow Y_M} \equiv k_Y \quad (13)$$

$$k_{X_A \to Y_A} = k_{X_M \to Y_M} \equiv k_Y \quad (14)$$

$$k_{Y_A \to X_A} = k_{Y_M \to X_M} \equiv k_Y + S_X. \quad (15)$$

Due to the term S_X, the whole system is kept in a non-equilibrium state. The last particle ($\mathbf{W}$) represents water that does not change into other particles. We assume that water and autocatalytic particles are hydrophilic particles that are repelled by membranes, and resource and waste particles are neutral particles which can diffuse through membranes.

The rate coefficients of spontaneous reactions are $k_A = k_M = 1.0 \times 10^{-8}$, $k_Y = 1.0 \times 10^{-4}$. The coefficients of catalytic activity are $C_A = 1.0 \times 10^{-5}$ and $C_M = 1.0 \times 10^{-5}$. The mutation rate is $\mu = 1.0 \times 10^{-12}$. The rate of resource supply is given a constant $S_X = 16$.

The simulation is based on a Metropolice method. At each iteration, the following steps are repeated,

1. Calculate the potential of each particle.

2. Calculate the probabilities of diffusion, rotation and chemical transition according to the potential difference.

3. Change the state of particles according to the probabilities synchronously.

In the initial state, the particles are placed randomly. There are 30 particles on a site on average, and the mean numbers of particles on a site are listed in Table 3. There is a sufficient number of resource particles and supplies to sustain metabolism. The average production rate of membranes is set very low at first. Catalysts with higher activity only emerge through random mutations. The reaction sites are arranged as a 64×64 triangular lattice whose boundaries are periodic.

Table 3: Mean numbers on a site in the initial state

particle	$\mathbf{A_0}$	$\mathbf{A_1}$	$\mathbf{A_2}$	$\mathbf{A_3}$	$\mathbf{A_4} \ldots \mathbf{A_9}$	
$\overline{n}_i$	1.6	1.2	0.8	0.4	0.0	
particle	$\mathbf{X_A}$	$\mathbf{Y_A}$	$\mathbf{M}$	$\mathbf{X_M}$	$\mathbf{Y_M}$	$\mathbf{W}$
$\overline{n}_i$	2.0	2.0	0.0	5.0	5.0	10.0

Simulation Results

The evolution of this system is roughly divided into three characteristic stages: (1) Chemical evolution, (2) Emergence of proto-cells, and (3) Cellular evolution.

Chemical Evolution

Fig. 3(1) shows the initial configuration. Before cellular selection starts, the chemical evolution simply depends on the reproduction rate of each species. In this model, because they share the same reproduction rate, the evolution is mostly driven by mutations and random fluctuation. At first, the largest part of the autocatalytic particles is $\mathbf{A_0}$ which does not produce membrane particles. Table 4 shows a profile of the population after 30,000 iterations for a single run. However, as the populations of other species increase, small pieces of membranes are gradually formed. (Fig. 3(2)).

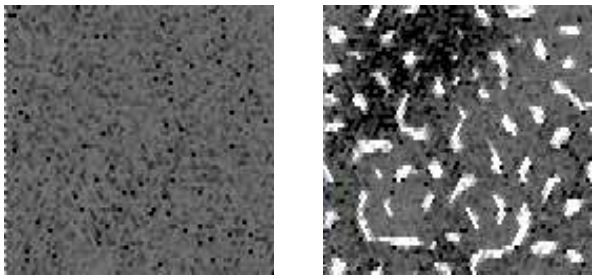

(1) Initial state (2) After 30,000 iterations

Figure 3: Chemical evolution. The white regions are dominated by particle $\mathbf{M}$. The depth of gray shade represents the total population of the autocatalysts ($\sum \mathbf{A_i}$). The black regions are dominated by particle $\mathbf{W}$. Resource and waste particles are not displayed in the figures. Pieces of membranes are produced by the catalysts which emerged through mutations.

Table 4: A profile of the population of particles after 30,000 iterations.

particle	$\mathbf{A_0}$	$\mathbf{A_1}$	$\mathbf{A_2}$	$\mathbf{A_3}$	$\mathbf{A_4}$
$\overline{n}_i$	1.00	0.60	0.42	0.20	0.05
particle	$\mathbf{A_5}$	$\mathbf{A_6}$	$\mathbf{A_7}$	$\mathbf{A_8}$	$\mathbf{A_9}$
$\overline{n}_i$	0.07	0.08	0.05	0.04	0.06
particle	$\mathbf{X_A}$	$\mathbf{Y_A}$	$\mathbf{M}$	$\mathbf{X_M}$	$\mathbf{Y_M}$
$\overline{n}_i$	3.00	4.43	1.57	3.68	4.77

Emergence of Proto-cells

Once membranes are formed, they begin to restrict the diffusion of catalysts. Thus, membranes can keep the local population and also their reaction rate high. As resource particles are consumed faster in such regions, resource particles diffuse into these regions according to the gradient of the population. It increases their reaction rate more. Due to this osmotic competition for resources, a small difference in the population of autocatalysts between the two sides of the membrane becomes larger.

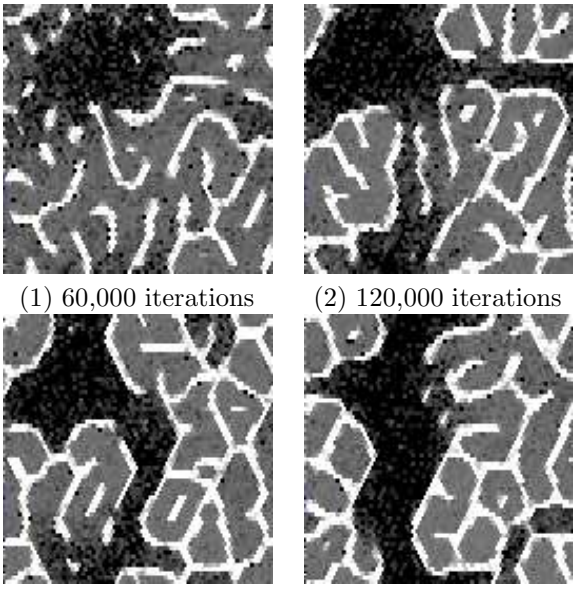

(1) 60,000 iterations (2) 120,000 iterations

(3) 180,000 iterations (4) 240,000 iterations

Figure 4: Emergence of Proto-cell structures. As the membranes grow, competition for resources between regions separated by membranes takes place. The regions differentiate into two states. In some regions that are enclosed by membranes, the density of autocatalysts stays high. In the other regions, their density becomes almost zero.

When the density of resources becomes too low in some regions, autocatalysts are no longer able to sustain their replication. Autocatalysts and membrane particles in these regions decay. At last, most regions become inactive, namely, filled with only resource and waste particles (and water), while there remain some active regions in which autocatalysts keep reproducing. These structures maintain themselves autopoietically, namely, the autocatalysts inside them reproduce themselves and metabolize the membrane particles to maintain their membranes. We call this structure a "proto-cell" hereafter.

Cellular Reproduction

A proto-cell can not only maintain itself but can reproduce itself. Figure 5 shows snapshots of the reproduction process. A proto-cell structure grows in size by assimilating resource particles from neighboring regions. As it grows, it comes to produce more membrane particles than it needs to maintain its membrane. When it reaches a certain size, surplus membrane particles begin to form another membrane inside the cell. This divides the mother cell into a few daughter cells. The daughter cells can continue to grow and reproduce recursively.

On the other hand, if a cell fails to maintain its membrane, the density of catalysts lowers quickly due to diffusion through the defect of membrane. When the density becomes too low, the catalysts can not sustain the metabolism any longer, and the whole structure finally disappears. This mutual dependency between membrane and metabolic system is essential to the evolution of proto-cells.

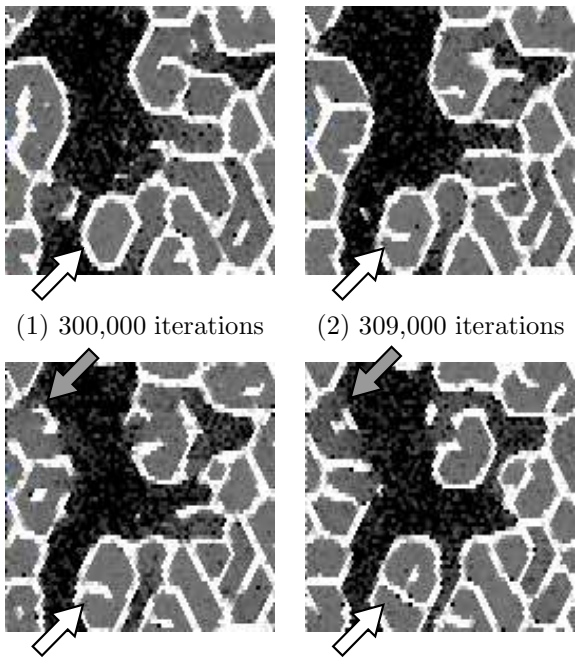

(1) 300,000 iterations (2) 309,000 iterations

(3) 318,000 iterations (4) 327,000 iterations

Figure 5: Reproduction of proto-cell. Snapshots from 300,000 iterations to 327,000 iterations. The proto-cell indicated by the white arrow grows gradually in size. When it becomes too large, another membrane appears inside it. At last, it divides the cell into daughter cells. On the other hand, the cell indicated by the gray arrows could not produce enough membrane particles to keep its membrane. Catalysts in the cell diffuse away through the defect of the membrane.

Selection of Catalysts Through Cellular Reproduction

Figure 6 shows the evolution of the population of catalysts. If there is no spatial structure, the populations of catalysts just randomly drift around the equilibrium where all populations are equal. However, once the differentiation into active and inactive regions has advanced, it becomes difficult to sustain metabolism without membranes, because the density of autocatalysts lowers fast.

Note that when a proto-cell divides itself, the composition of the population of replicators contained in the cell is roughly inherited by the daughter cells. This implies that catalysts that can sustain a proto-cell more stably are selected regarding a proto-cell as a new unit of Darwinian evolution. Therefore, due to cellular selection,

the populations of catalysts are biased toward higher membrane production activity against the random drift. The populations of catalysts and their relative amount ($\rho_i = \overline{n_i} / \sum \overline{n_j} \times 100$) after 600,000 iterations for the same run as the previous one are listed in Table 5.

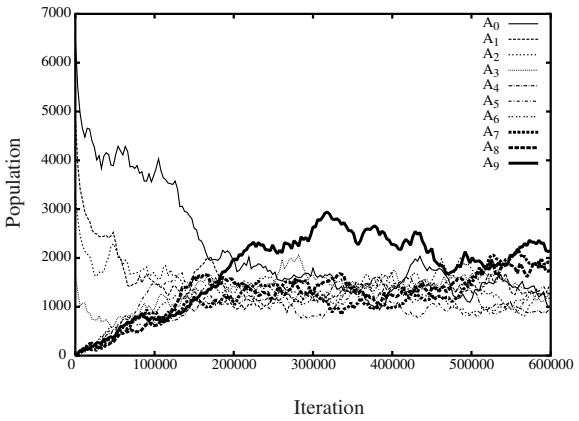

Figure 6: Evolution of the population of autocatalysts. At first, the population of $\mathbf{A_0}$, which does not produce membrane particles, is the largest. However, other species arise through mutation, and after the formation of proto-cells, species which can produce membranes have an advantage over $\mathbf{A_0}$ (see the thick lines which denote species $\mathbf{A_7}$ – $\mathbf{A_9}$).

Table 5: A profile of the populations of catalysts after 600,000 iterations.

particle	$\mathbf{A_0}$	$\mathbf{A_1}$	$\mathbf{A_2}$	$\mathbf{A_3}$	$\mathbf{A_4}$
$\overline{n}_i$	0.24	0.36	0.28	0.30	0.23
$\rho_i(\%)$	7.0	10.5	8.1	8.7	6.7
particle	$\mathbf{A_5}$	$\mathbf{A_6}$	$\mathbf{A_7}$	$\mathbf{A_8}$	$\mathbf{A_9}$
$\overline{n}_i$	0.31	0.31	0.46	0.43	0.52
$\rho_i(\%)$	9.0	9.0	13.4	12.5	15.1

To make the effects of the cellular selection more clear, we investigated evolution under a lower resource supply. The initial configuration and the parameters are the same as those of the previous run. After the formation of the proto-cell structures (after 300,000 iterations), the rate of resource supply S_X was decreased to $S_X \times 0.75$. Because the density of resource particles decreases, catalysts have to keep their density high to maintain a sufficient reproduction rate more tightly, and a cell that fails to maintain its membrane disappears faster. The pressure to acquire higher membrane production activity becomes stronger. Table 6 shows the populations after 900,000 iterations for another run. The dominance of catalysts with higher activity is clearer.

To see the detailed process of cellular selection, the evolution of the mean activity ($\overline{C_{M_i}} = \sum C_{M_i} N_{A_i} / \sum N_{A_i}$) of membrane production is shown in Fig. 7. Within a cell, because competition among the autocatalysts is neutral, the mean activity of each cell fluctuates randomly. But among the cellular assembly, a proto-cell in which membrane production activity is low becomes extinct more often. As a result, cells with higher catalytic activity outperform the lower ones and the total average of $\overline{C_{M_i}}$ gradually increases.

Table 6: A profile of populations after 900,000 iterations under the lower resource supply.

particle	$\mathbf{A_0}$	$\mathbf{A_1}$	$\mathbf{A_2}$	$\mathbf{A_3}$	$\mathbf{A_4}$
$\overline{n}_i$	0.19	0.10	0.11	0.16	0.13
$\rho_i(\%)$	8.6	4.5	5.0	7.3	5.9
particle	$\mathbf{A_5}$	$\mathbf{A_6}$	$\mathbf{A_7}$	$\mathbf{A_8}$	$\mathbf{A_9}$
$\overline{n}_i$	0.18	0.25	0.20	0.42	0.46
$\rho_i(\%)$	8.2	11.4	9.1	19.1	20.9

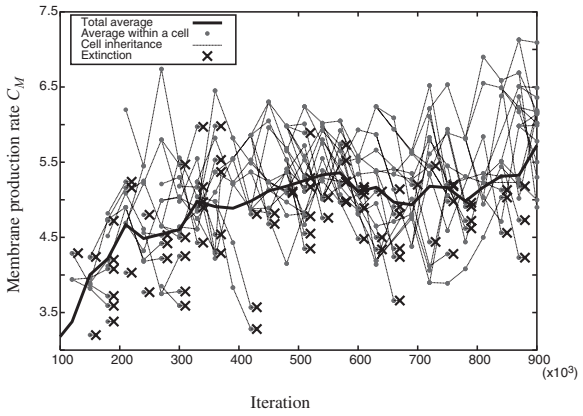

Figure 7: Evolution of the mean activity of membrane production ($\overline{C_{M_i}}$). A cell with lower membrane production breaks more often because its membrane is weaker.

Though there often appear cells with very high activity of membrane production, the $\overline{C_{M_i}}$ of these cells soon drops again. These drops are caused by the invasion of "parasitic" catalysts. Namely, the evolved cells are dominated by catalysts that have higher activity and produce enough membrane particles, however, the catalysts with lower activity, e.g., $\mathbf{A_0}$, can always emerge through mutation and increase through the random fluctuation within these cells. Snapshots of the process of cellular selection are shown in Fig. 8. At 780,000 iterations, the cells indicated by the white arrows are deeply infected by parasites. It becomes difficult for these cells to maintain their membranes and they disappear before 900,000 iterations. The cells at 900,000 iterations are produced from survived cells that have higher catalytic activity, but, there are cells that are newly invaded by

parasites (indicated by the gray arrow). This result indicates that these proto-cells have limited "life spans". A proto-cell has to keep dividing itself to escape from parasites, otherwise, the parasitic catalysts increase in it before long.

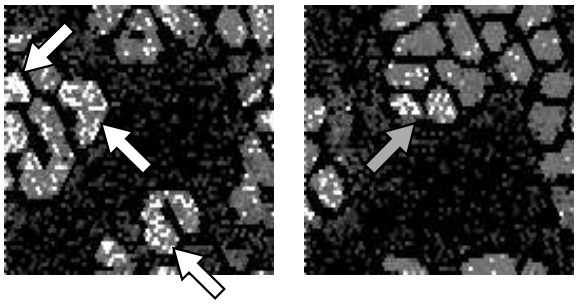

(1) 780,000 iterations (2) 900,000 iterations

Figure 8: Invasion of parasitic catalysts. The white sites are where the mean catalytic activity is low.

As the cellular evolution proceeds, it is observed that the size of the cells becomes smaller. Figure 9 shows a histogram of cell sizes (namely, the number of sites within the membranes) for the same run, after 300,000, 600,000 and 900,000 iterations. The mean sizes of cells at each iteration are 103.8, 82.7, and 66.2, respectively. When the mean activity of the membrane production of a cell increases, it can maintain its membrane with fewer catalysts, and it can divide itself faster. However, it is sometimes observed that a cell whose size is too small fails to maintain itself. When a cell produces too many membrane particles or the size of cell become too small, the rate of replication of the autocatalysts decreases, because the hydrophobic environment suppress the synthesis of hydrophilic particles. A certain optimum size of the cell will be achieved through the selection of catalysts. This expectation is supported by the result that, in the evolved state, the dispersion of cell sizes becomes smaller.

Conclusion and Discussion

In this article, we have presented a model for the evolution from molecular to cellular reproduction. Starting from a homogeneous, random initial state, we demonstrated the emergence of proto-cells. This goes through three stages: (1) Metabolic cycles that produce membrane molecules can arise through pre-cellular chemical evolution. (2) Proto-cell structures, i.e., self-maintaining structures that maintain their own membranes by themselves emerge spontaneously. (3) A proto-cell structure reproduces itself. Because the molecules contained inside a proto-cell can pass genetic information into daughter cells, it can be regarded as a unit of Darwinian evolution. Cells that can maintain themselves more stably evolve through cellular selection.

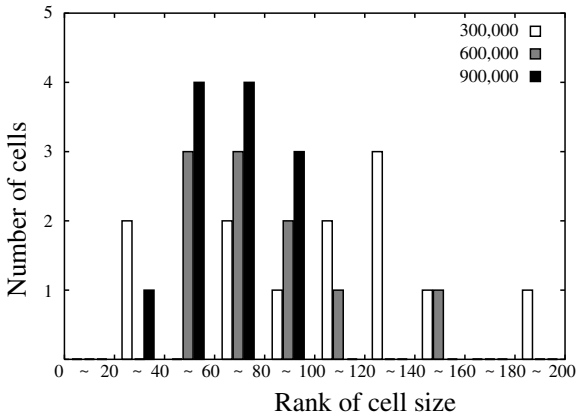

Figure 9: The distribution of cell sizes after 300,000, 600,000 and 900,000 iterations. The standard deviations of the sizes are 47.52, 26.58,and 24.26, respectively.

Excess production of membrane particles generates a hydrophobic environment, which is less optimal for the self-reproduction of the particles. Nevertheless, particles with higher catalytic ability replicate more via cellular level selection. As a result, the average value of catalyzation with membrane formation becomes higher than that without membrane formation. We insist here that the emergence of cellular structures produces a new rugged evolutionary landscape on the particle level.

The entire behavior is insensitive to parameter values whenever we have the conditions of, 1) a membrane formation and 2) transportation of resource particles through membranes. This robust behavior gives an advantage to our model over other cellular formation systems such as Grey-Scott, whose spatio-temporal pattern is sensitive to reaction and diffusion rates. In our model, the size of cells and replication rates change but their qualitative behaviors never change. Instead, our model behavior is sensitive to the form of repulsion potential of the membrane particles. In this study, we chose a set of values which provide flexible membranes to make the organization of proto-cells easier. We take the advantage of this sensitivity to the potential form in order to study the evolutionary dynamics of these characteristics of membranes of proto-cells.

In the simulations reported here, the resources supply was homogeneous. And the pressure to evolve membrane production became clear when the resource supply rate was lowered. These results suggest that, if the supply of resource is not homogeneous, namely, if there is a small region where the resource supply is plenty enough to sustain metabolism, but the supply is rather poor in the other regions, pre-cellular evolution will take place where the resource supply is high enough, and once the proto-cell structures are acquired, they can migrate where the resource supply is lower, which will promote the further

evolution of cellular structures.

Though the model introduced in this article is simple and abstract, we are now extending our model to implement more complex metabolic reactions that can produce more diverse membrane particles and various cell types. Our next objective is to investigate the co-evolution of metabolic systems and cellular structures. Because in our model, the birth and death of cells are all actualized through the elemental interactions of particles, without any ad-hoc rules, the way in which the proto-cell is organized itself can evolve. In this sense, it can be regarded as a basic model for the organization of a dynamical hierarchy. We expect that higher order structures (e.g., cell differentiation and cooperative interaction between cells) are yielded.

Furthermore, the dynamics of our model is based on a local equilibrium system. A quantitative analysis of this model may bring insight to the evolution of primitive cells as a non-equilibrium system from a thermodynamical aspect. Along these lines, computational models of artificial chemistry will provide useful tools for understanding the earliest evolution of life.

Acknowledgments

This work was partially supported by the COE project ("complex systems theory of life"), a Grant-in-aid (No. 11837003) from the Ministry of Education, Science, Sports and Culture and afiis project (Academic Frontier, Intelligent Information Science 2000 - 2004 Doshisha University).

References

Breyer, J.; Ackermann, J.; and McCaskill, J. 1998. Evolving reaction-diffusion ecosystems with self-assembling structures in thin films. *Artificial Life* 4:25–40.

Gánti, T. 1975. Organization of chemical reactions into dividing and metabolizing units: The chemotons. *BioSystems* 7:15–21.

Gánti, T. 1997. Biogenesis itself. *J. theol. Biol.* 187:583–593.

Maturana, H. R., and Varela, F. J. 1980. *Autopoiesis and Cognition: the Realization of the Living.* D. Reidel Publishing.

McMullin, B., and Varela, F. J. 1997. Rediscovering computational autopoiesis. In Husbands, P., and Harvey, I., eds., *4th European Conference on Artificial Life*, 38–47. Brighton, UK: MIT press.

Ono, N., and Ikegami, T. 1999. Model of self-replicating cell capable of self-maintenance. In Floreano, D.; Nicoud, J. D.; and Mondada, F., eds., *Proceedings of the 5th European Conference on Artificial Life (ECAL'99)*, 399–406. Lausanne, Switzerland: Springer.

Ono, N., and Ikegami, T. 2001. Artificial chemistry: Computational studies on the emergence of self-reproducing units. In Kelemen, J., and Sosik, S., eds., *Proceedings of the 6th European Conference on Artificial Life (ECAL'01)*, 186–195. Prague, Czech Republic: Springer.

Speroni di Fenizio, P.; Dittrich, P.; and Banzhaf, W. 2001. Spontaneous formation of proto-cells in a universal artificial chemistry of a planar graph. In Kelemen, J., and Sosik, S., eds., *Proceedings of the 6th European Conference on Artificial Life (ECAL'01)*, 206–215. Prague, Czech Republic: Springer.

Szathmáry, E., and Maynard Smith, J. 1997. From replicators to reproducers: the first major transitions leading to life. *J. theor. Biol* 187:555–571.

Varela, F. J.; Maturana, H. R.; and Uribe, R. 1974. Autopoiesis: The organization of living systems, its characterization and a model. *BioSystems* 5:187–196.

Zeleny, M. 1977. Self-organization of living systems: A formal model of autopoiesis. *International Journal of General Science* 4:13–28.